

EMC Coupling Between Two Composite Right/Left-Handed (CRLH) Transmission Lines on PCBs

Irfanullah, Shahid Khattak, and Imdad Khan

Department of Electrical and Computer Engineering
COMSATS University Islamabad, Abbottabad Campus, Pakistan
eenr@cuiatd.edu.pk

Abstract — Unintentional electromagnetic coupling (crosstalk) between PCB lands is an important aspect of the design of an electromagnetically compatible product. In this paper, analytical model to predict crosstalk between two composite right/left-handed (CRLH) transmission lines in close proximity on PCBs is developed, and validated with full-wave simulation and measurement results. A cascaded seven unit cells CRLH transmission line (TL) acting as source of the electromagnetic emission was placed in close proximity to another seven unit cells CRLH transmission line acting as receptor of the emission on PCBs. Then the near- and far-end crosstalk voltages induced from the generator CRLH-TL to receptor TL for various separations between them were analyzed. It is shown that the crosstalk voltages computed with developed analytical model agrees well with full-wave simulation and measured results. Furthermore, it is shown that the left-handed capacitance and inductance design parameters of CRLH-TL can be used to reduce the crosstalk voltages induced on the receptor circuit leading to a cost-effective solution for shielding of near-by CRLH-TL receptor circuits printed on PCBs for various engineering applications.

Index Terms — CRLH, crosstalk, coupler, EMC.

I. INTRODUCTION

An important aspect of the design of an electromagnetically compatible product is crosstalk. This essentially refers to the unintended electromagnetic coupling between wires and PCB lands that are in close proximity. The crosstalk analysis (i.e., to determine the near-end and far-end voltages) between conventional coupled cables and coupled PCB lands has been widely studied in the literature, see for example [1-3, 16-18]. Recently, characteristics of the composite right/left-handed (CRLH) metamaterial transmission lines (MTM-TLs) from intentional/tight coupling point of view (for example directional couplers) has been investigated [4-6]. While a lot of attention has been paid to the intentional coupling between CRLH-TLs, not much work (except in [7]) has been done on these couplers

from an unwanted electromagnetic compatibility (EMC) coupling perspective. In the research community there is a growing interest to use CRLH-TLs in the design of feed network for antenna arrays [8-10], particularly by placing multiple RH/CRLH-TLs in the feed network to obtain different polarizations [11]. In such scenarios, unwanted coupling from one TL to another can degrade the systems' performance by deteriorating the desired radiation patterns. Similarly multiple coupled CRLH-TLs have been realized in super-resolution imaging applications [12]. Therefore analysis of crosstalk voltages to mitigate mutual coupling is an important design parameter to obtain the desired performance metrics. In [7], analysis of noise voltage coupling between right-handed (RH) and CRLH-TLs has been formulated.

The research work in the paper differs from previous work as follows: In [4]-[6] coupling between CRLH-TLs has been investigated from intentional coupling point of view, that is to couple more power to the receptor TL (ideally 0 dB). In the proposed work, coupling from EMC point of view has been analyzed, that is the objective is to mitigate the coupled voltages from generator CRLH-TL to the receptor CRLH-TL. The work in [7] assumes weak coupling between RH-TL and CRLH-TL, that is the effects of coupling only from generator RH-TL to victim CRLH-TL has been considered and not the effects of coupling back from CRLH-TL to RH-TL has been included. In [1-2 and 7], derivations of NEXT and FEXT is done with the assumptions of weak coupling between coupled transmission lines, and therefore the models cannot predict the crosstalk voltages for strong coupling between the PCB lands, where the transmission lines are printed in close proximity on the printed boards. In contrast to [7], the proposed work here considers the two-way effects of mutual coupling (coupling from generator CRLH-TL to receptor CRLH-TL and back to the generator circuit by the receptor circuit) to compute crosstalk voltages. Therefore, the proposed crosstalk model predicts the near- and far-end coupled voltages for any arbitrary spacing between the coupled transmission lines. Different commercially available simulators are

available to analyze the crosstalk between transmission lines of different structures. However, these techniques are based on method of moments (MoM), finite difference time domain (FDTD) numerical techniques [19] which are computationally expensive, time consuming and needs large amount of memory to analyze the crosstalk, particularly for complex transmission structures. In addition, they do not give insight behavior and relationship of crosstalk noise voltages with different parameters of the coupled transmission lines. The frequency domain analytical model proposed in this work to derive expressions for near- and far-end crosstalk voltages is generic and can be applied to other complex coupled transmission lines on printed circuit boards for any arbitrary spacing in between them. The analytical expressions developed can be used as an aiding tools for theoretical support, validation, comparison and design guidelines for reducing the unintentional coupling from generator to receptor circuit or vice-versa.

Rest of the paper is organized as follows: In Section II, analytical expressions to compute NEXT and FEXT voltages for a unit-cell coupled CRLH-TLs have been derived. Section III describes the simulation methodology to validate the derived analytical expressions. Section III also discusses the parametric study of left-handed parameters C_L and L_L on NEXT and FEXT voltages. Section IV describes the measurement procedure to compute the crosstalk voltages and Section V finally concludes the paper.

II. DERIVATION OF ANALYTICAL EXPRESSIONS TO COMPUTE NEXT AND FEXT VOLTAGES

To introduce the problem statement, consider the coupled unit-cell CRLH-CRLH TL shown in Fig. 1 (a), and its equivalent circuit model [15] shown in Fig. 1 (b). The microstrip Interdigital capacitor comprising of ten long conductors (or fingers), each having length L_f and width W_f is represented by left-handed (LH) series capacitance (C_L) in series with a right-handed (RH) parasitic inductance (L_R). The shunted stub (shorted with a metallic via) having length L_s and width W_s is represented by LH shunt inductance (L_L) in parallel with a RH parasitic capacitance (C_R). L_{GR} and C_{GR} represents mutual inductance and mutual capacitance between generator and receptor circuits respectively. To introduce the two-way effects of mutual coupling, dependent voltage sources in the generator and receptor circuits have been incorporated as shown in Fig. 1 (b). The dependent voltage source $sL_{GR}I_G$ in the receptor circuit represents the effects of generator current and the dependent voltage source $sL_{GR}I_R$ in the generator circuit represents the back-way effect of receptor current, where by definition $= j\omega$. Port 1 is driven by the voltage source

V_s , ports 2, 3 and 4 are terminated by load resistance R_L , near-end resistance R_{NE} and far-end resistance R_{FE} respectively.

Next, the goal is to derive analytical expressions to determine near-end crosstalk (NEXT) voltage V_{NE} and far-end crosstalk (FEXT) voltage V_{FE} . In [7], analytical expressions for NEXT and FEXT voltages have been derived using weak coupling assumptions, while the proposed coupling model here in Fig. 1 (b) will be considered in entirety without weak coupling assumptions. Then design guidelines will be provided by parametric study of the left-handed parameters L_L and C_L in the receptor circuit for mitigation of NEXT and FEXT voltages.

To determine NEXT voltage V_{NE} and FEXT voltage V_{FE} in Fig. 1 (b), the generator and receptor currents are given by:

$$I_G = \frac{V_4 - V_1}{sL_R + \frac{1}{sC_L}} = \frac{sC_L(V_4 - V_1)}{1 + s^2 L_R C_L} = A(V_4 - V_1), \quad (1)$$

$$I_R = \frac{V_2 - V_3}{sL_R + \frac{1}{sC_L}} = \frac{sC_L(V_2 - V_3)}{1 + s^2 L_R C_L} = A(V_2 - V_3), \quad (2)$$

$$\text{where } A = \frac{sC_L}{1 + s^2 L_R C_L}. \quad (3)$$

and V_1, V_2, V_3, V_4 are node voltages in Fig. 1 (b).

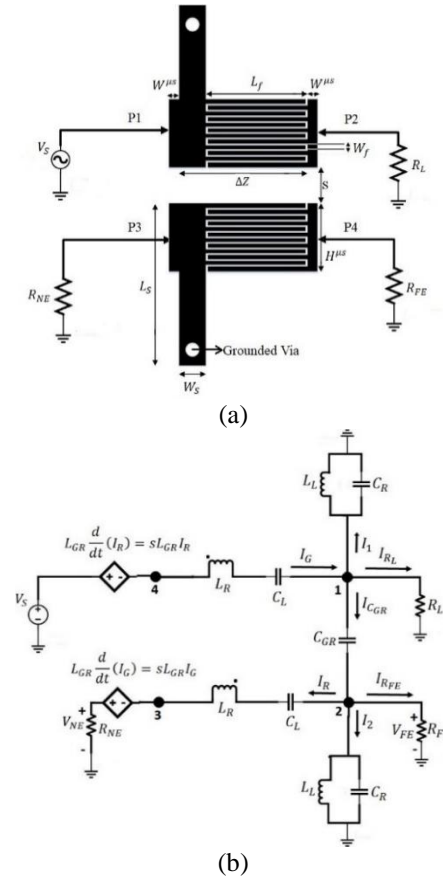


Fig. 1. (a) Microstrip layout of a unit-cell CRLH-CRLH coupler, (b) Proposed equivalent circuit model of the unit-cell CRLH-CRLH coupler.

Applying KCL at node 1: $I_G = I_{C_{GR}} + I_1 + I_{R_L}$, (4)

or

$$A(V_4 - V_1) = (V_1 - V_2)sC_{GR} + \frac{V_1}{\frac{1}{sC_{GR} + \frac{1}{sL_L}} + \frac{V_1}{R_L}}. \quad (5)$$

Let,

$$B = \frac{1}{sC_{GR} + \frac{1}{sL_L}}, \quad (6)$$

and then re-arranging (5), we get:

$$\left(-A - B - sC_{GR} - \frac{1}{R_L}\right)V_1 + sC_{GR}V_2 + AV_4 = 0. \quad (7)$$

Applying KVL around V_s and node 4 in Fig. 1 (c), we can write:

$$V_s - sL_{GR}I_R - V_4 = 0. \quad (8)$$

Using (2) and (8) in (7), and re-arranging, we obtain:

$$\left(-A - sC_{GR} - B - \frac{1}{R_L}\right)V_1 + (sC_{GR} - sL_{GR}A^2)V_2 + sL_{GR}A^2V_3 + AV_s = 0. \quad (9)$$

Similarly, applying KCL and KVL at nodes 2 and 3 respectively in the receptor circuit, we obtain:

$$sC_{GR}V_1 + \left(-A - B - sC_{GR} - \frac{1}{R_{FE}}\right)V_2 + AV_3 = 0, \quad (10)$$

$$-sL_{GR}AV_1 + (AR_{NE} - s^2L_{GR}^2A^2)V_2 + (-AR_{NE} - 1 + s^2L_{GR}^2A^2)V_3 + sL_{GR}AV_s = 0. \quad (11)$$

Suppose,

$$K_1 = -A - sC_{GR} - B - \frac{1}{R_L}, K_2 = sC_{GR} - sL_{GR}A^2, K_3 = sL_{GR}A^2, K_4 = -sC_{GR} - \frac{1}{R_{FE}} - A - B, K_5 = AR_{NE} - s^2L_{GR}^2A^2, K_6 = -AR_{NE} - 1 + s^2L_{GR}^2A^2. \quad (12)$$

Then (9), (10) and (12) becomes:

$$K_1V_1 + K_2V_2 + K_3V_3 + AV_s = 0, \quad (13)$$

$$sC_{GR}V_1 + K_4V_2 + AV_3 = 0, \quad (14)$$

$$-sL_{GR}AV_1 + K_5V_2 + K_6V_3 + sL_{GR}AV_s = 0. \quad (15)$$

Solving (13), (14) and (15) simultaneously, we can compute V_2 , and V_3 to find out NEXT and FEXT voltages as follows:

$$V_2 = \frac{-AV_s}{M_1} - \frac{M_2(M_3 - sL_{GR}M_1)AV_s}{M_1(M_1M_4 - M_2M_3)}, \quad (16)$$

$$V_3 = \frac{(M_3 - sL_{GR}M_1)AV_s}{M_1M_4 - M_2M_3}, \quad (17)$$

where

$$M_1 = \frac{(K_1 - sC_{GR})(sC_{GR} - K_2)}{sC_{GR}} + (sC_{GR} - sL_{GR}A^2), M_2 = sL_{GR}A^2 - \frac{A(K_1 - sC_{GR})}{sC_{GR}}, M_3 = -sL_{GR}A + \frac{AK_2L_{GR}}{C_{GR}} + AR_{NE} - s^2L_{GR}^2A^2, M_4 = \frac{L_{GR}}{C_{GR}}A^2 - AR_{NE} - 1 + s^2L_{GR}^2A^2. \quad (18)$$

The NEXT voltage is given by:

$$V_{NE} = I_{R_{NE}}R_{NE} = A(V_2 - V_3)R_{NE}, \quad (19)$$

where A can be computed from (3) and V_2 , V_3 can be determined using (16) and (17). The FEXT voltage is given by:

$$V_{FE} = I_{R_{FE}}R_{FE} = V_2. \quad (20)$$

Notice that the expressions in (19) and (20) are complex and depends on circuit parameters in Fig. 1 as well on frequency, indicating the generality of the

expressions.

III. SIMULATION METHODOLOGY

A. NEXT and FEXT voltages for unit-cell CRLH-CRLH coupling

In this section, a unit-cell CRLH-CRLH coupler of Fig. 1 is used to validate the previously derived NEXT and FEXT voltages in (19) and (20) in both Momentum (Fig. 1 (a)) and circuit simulator (Fig. 1 (b)) of ADS. The unit-cell coupler was simulated with port 1 driven by voltage source $V_s = 1$ V and ports 2, 3, and 4 were terminated with $R_L = 50\Omega$, $R_{NE} = 50\Omega$, and $R_{FE} = 50\Omega$ terminations respectively. The circuit parameter values chosen were $L_R = 1.76$ nH, $C_R = 0.53$ pF, $L_L = 0.47$ nH, $C_L = 0.55$ pF. These circuit values were extracted for the unit-cell microstrip CRLH-TL shown in Fig. 1 (a) using the design procedure in [13] with the following parameters: $L_f = 5$ mm, $W_f = 0.3$ mm, $L_s = 10$ mm, $W_s = 2$ mm and all spacing between fingers of 0.2 mm. Two extra small microstrip transmission lines with dimensions $H^{\mu s} = 4.8$ mm, $W^{\mu s} = 1$ mm were added at both ends of the structure for matching and feeding purpose and their effects must be excluded by de-embedding (extending the ports P1 and P2 to the structure in the simulator). The methodology of parameters extraction is based on ABCD parameters approach explained in [13] and outlined here briefly:

1) Simulate Interdigital capacitor (IDC) separately to extract its S-parameters at three frequencies, namely design frequency f_0 and two edge frequencies f_1 and f_2 around f_0 . In this paper, the chosen values were $f_0 = 3$ GHz, $f_1 = 2.9$ GHz and $f_2 = 3.1$ GHz.

2) Repeat step 1 for shunted stub inductor.

3) Convert S-parameters into Z and Y parameters.

4) Use following expressions to compute circuit values [4],

$$L_R = L_s^{IDC}, C_R = 2C_p^{IDC} + C_p^{stub}, L_L = L_p^{stub}, C_L = C_s^{IDC}, \quad (21)$$

where

$$C_p^{IDC} = \frac{Y_{11}^{IDC} + Y_{21}^{IDC}}{j\omega}, L_s^{IDC} = \frac{1}{2j\omega} \left[\omega \frac{\partial \left(\frac{1}{Y_{21}^{IDC}} \right)}{\partial \omega} + \frac{1}{Y_{21}^{IDC}} \right], C_s^{IDC} = \frac{2}{j\omega} \left[\omega \frac{\partial \left(\frac{1}{Y_{21}^{IDC}} \right)}{\partial \omega} - \frac{1}{Y_{21}^{IDC}} \right]^{-1}, L_s^{stub} = \frac{Z_{11}^{stub} - Z_{21}^{stub}}{j\omega}, C_p^{stub} = \frac{1}{2j\omega} \left[\omega \frac{\partial (Y_{21}^{stub})}{\partial \omega} + Y_{21}^{stub} \right], L_p^{stub} = \frac{2}{j\omega} \left[\omega \frac{\partial (Y_{21}^{stub})}{\partial \omega} - Y_{21}^{stub} \right]^{-1}. \quad (22)$$

All the values to be computed at ω_0 and $\frac{\partial(Y)}{\partial\omega} \cong \frac{Y_{at\omega_2} - Y_{at\omega_1}}{\omega_2 - \omega_1}$.

The values of mutual coupling parameters L_{GR} and C_{GR} were computed by first simulating the unit-cell

CRLH-CRLH coupler in ADS Momentum and then tuning the parameters L_{GR} and C_{GR} in ADS schematic to match the results with the Momentum results. The extracted parameters corresponding to 3 mm edge to edge separation between the unit-cell CRLH-CRLH coupler are $L_{GR} = 1.04$ nH and $C_{GR} = 0.8$ pF. The separation of 3 mm was chosen to investigate the strong coupling case between CRLH-CRLH coupler. A weak coupling case with separation of 10 mm has also been investigated in Section IV. The ADS circuit (using Fig. 1 (b)), ADS Momentum (using Fig. 1 (a)) and MATLAB analytical results using (19) and (20) with these extracted parameters are shown in Fig. 2. The analytical and circuit simulation results completely overlap each other, which validates the accuracy of (19) and (20) for computation of NEXT and FEXT voltages. It can be seen that the behavior of NEXT and FEXT voltages is similar except for the frequency range of 2-3 GHz, which is a left-hand propagation band of CRLH-TL. It is shown in [13] that the near-end coupling is increased in the left-hand propagation band due to opposite direction of Poynting vector (power flow) and propagation vector. Therefore in next sections, only results for NEXT voltage would be discussed.

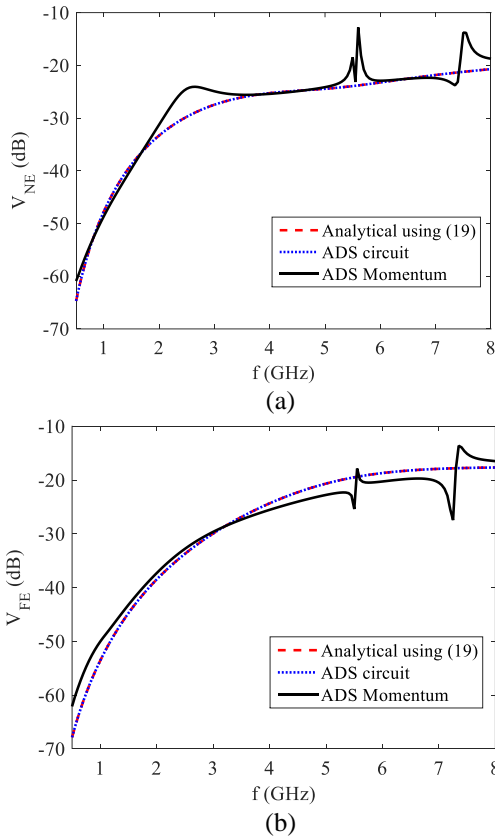


Fig. 2. Comparison of the analytical (MATLAB), ADS circuit simulation and ADS Momentum for: (a) NEXT and (b) FEXT voltages of unit-cell (UC) CRLH-CRLH coupler.

B. Parametric study of left-handed parameters

Next, to consider a more practical realization of EMC coupling, seven unit-cells of microstrip CRLH-CRLH coupler in Fig. 1 (a) were cascaded in ADS Momentum (3D planar EM simulator). The ADS Momentum results for NEXT voltages using 3 mm edge-to-edge separation between two seven unit-cells CRLH-TLs for various parameters are shown in Figs. 3 and 4. The parametric study is mainly focussed on the left-hand (LH) band of CRLH-TL, which is a band extending from high pass left-hand cutoff frequency (f_{CL}) to transition frequency (f_0). The f_{CL} represents the lowest frequency above which the CRLH-TL will support left-handed propagation, and f_0 represents the frequency at which the CRLH-TL transitions from supporting left-handed propagation to right-handed (RH) propagation. These frequencies are computed using the following expressions [13]:

$$f_{CL} = f_0 \sqrt{\frac{P_1 - P_2}{2}}, \quad (23)$$

where

$$P_1 = \left[K + \left(\frac{2}{\omega_L} \right)^2 \right] \omega_0^2, \quad P_2 = f_0 \sqrt{P_1^2 - 4}, \quad (23a)$$

$$f_0 = \frac{1}{2\pi \sqrt{L_R C_R L_L C_L}}, \quad f_L = \frac{1}{2\pi \sqrt{L_L C_L}}, \quad (23b)$$

$$\text{and } K = L_R C_L + L_L C_R. \quad (23c)$$

These cut-off and transition frequencies along with extracted circuit parameters are shown in Tables 1 and 2.

1) Effects of finger length (L_f) on NEXT voltage

To investigate the effects of finger length (L_f) in Fig. 1 (a) on NEXT voltage in left-hand (LH) band, two seven unit-cells CRLH-CRLH TL coupler with edge to edge separation of 3 mm (strong coupling case) was simulated in ADS Momentum. The extracted circuit parameters and LH band for various finger lengths are shown in Table 1. These values were computed using the simulation methodology in Section III and using equations (23). The NEXT voltage for various values of L_f is shown in Fig. 3. Other parameters of Fig. 1 (a) were $W_f = 0.3$ mm, $L_s = 10$ mm, $W_s = 2$ mm and all spacing in the fingers of 0.2 mm. As can be seen in Table 1, by increasing the finger length, the cut-off frequency f_{CL} is decreased resulting in shifting the LH band towards the lower frequency and can also be observed in Fig. 3. The NEXT voltage stays maximum up to around -10 dB for frequencies above 3 GHz and it is below -20 dB for frequencies below 3 GHz for all values of L_f in both LH and RH bands.

2) Effects of stub width (W_s) on NEXT voltage

Similarly the NEXT voltage was investigated for different values of stub width (W_s) and the results are shown in Table 2 and Fig. 4. Other parameters of Fig. 1 (a) were $L_f = 5$ mm, $W_f = 0.3$ mm, $L_s = 10$ mm and all spacing in the fingers of 0.2 mm. As can be seen in Table 2, the bandwidth of LH band decreases from

3.74 GHz (for $W_s = 2$ mm) to 2.77 GHz (for $W_s = 6$ mm). The value of NEXT voltage increases for increasing value of W_s and is approximately 10 dB higher for $W_s = 6$ mm than for $W_s = 2$ mm in both LH and RH bands. This is an important investigation for reducing NEXT voltages in LH and RH bands of coupled CRLH TLs, which should be kept in mind while deigning CRLH-TLs for EMC coupling reduction.

Table 1: Extracted parameters for various finger lengths using (21)

| L_f (mm) | C_L (pF) | L_R (nH) | L_L (nH) | C_R (pF) | LH band ($f_{CL} - f_0$) |
|---------------|---------------|---------------|---------------|---------------|-------------------------------|
| 5 | 0.55 | 1.76 | 0.47 | 0.53 | 3.44 – 7.18 |
| 7 | 0.85 | 2.24 | 0.47 | 0.53 | 2.64 – 6.06 |
| 9 | 1.13 | 2.75 | 0.47 | 0.53 | 2.17 – 5.36 |

Table 2: Extracted parameters for various stub widths using (21)

| W_s (mm) | C_L (pF) | L_R (nH) | L_L (nH) | C_R (pF) | LH band ($f_{CL} - f_0$) |
|---------------|---------------|---------------|---------------|---------------|-------------------------------|
| 2 | 0.55 | 1.76 | 0.47 | 0.53 | 3.44 – 7.18 |
| 4 | 0.55 | 1.76 | 0.96 | 0.69 | 2.66 – 5.62 |
| 6 | 0.55 | 1.76 | 1.27 | 0.75 | 2.36 – 5.13 |

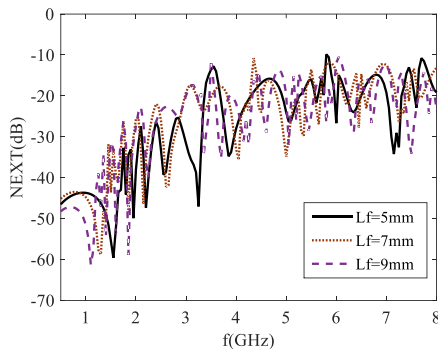


Fig. 3. Effects of length of finger (L_f) on NEXT voltage between two seven unit-cells CRLH-CRLH coupler in ADS Momentum.

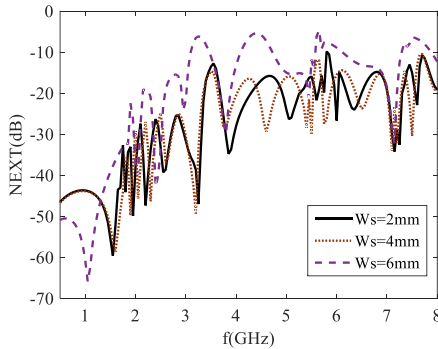
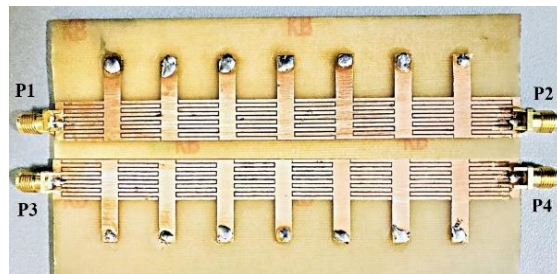


Fig. 4. Effects of width of stub (W_s) on NEXT voltage between two seven unit-cells CRLH-CRLH coupler in ADS Momentum.

IV. MEASUREMENT PROCEDURE AND RESULTS

Next, to measure the NEXT voltage between two 7 unit-cells CRLH-CRLH coupler TLs, two test cases were considered: case 1: edge to edge separation between TLs of 3 mm (strong coupling case) and case 2: edge to edge separation between TLs of 10 mm (weak coupling case). The two cases were printed on a 1.575 mm thick Rogers RT/duroid 5880 ($\epsilon_r = 2.2, \tan\delta = 0.0009$) substrate and are shown in Fig. 5 for cases 1 and 2 respectively. The specified dimensions denoted with notations in Fig. 1 (a) are $H^{\mu s} = 4.8$ mm, $W^{\mu s} = 1$ mm, $L_f = 5$ mm, $W_f = 0.3$ mm, $L_s = 10$ mm, $W_s = 2$ mm and all spacing in the fingers of 0.2 mm. These are the same values as were discussed in Section III. The measurement procedure is as follows and also mentioned in [1]: P1 (driven port) of the manufactured boards in Fig. 5 was connected with port 1 of the network analyzer, P3 (near-end port) was connected with port 3 of the network analyzer and P2 (load), P4 (far-end port) were terminated with 50Ω terminations. Then near-end crosstalk was measured from P1 to P3. Next, again P1 was connected with port 1 of the network analyzer, P4 with port 4 of the network analyzer and P2 and P3 were terminated with 50Ω terminations. Then far-end crosstalk was measured from P1 to P4. In-house fully calibrated Agilent four port network analyzer (300 kHz-20 GHz, model E5071C) was used for measurements purpose. The measured, circuit and ADS Momentum simulated results for the two cases are shown in Figs. 6 and 7 and are in good agreement. Cross-correlation metric has always been used for determining the similarity between two data series. Its value when normalized between -1 and 1 is called the correlation coefficient ρ which is a more meaningful measure of similarity between two data series. The results in the Table 3 give ρ values obtained between the proposed circuit method to that of the momentum method and the measured values for two data sets. Very high ρ values ranging from 0.97 to 0.974 indicate a very high degree of correlation between the results. The analytical expressions obtained in (19) and (20) can also be used directly to compute the crosstalk voltages (NEXT and FEXT) as was demonstrated in Section III.A.



(a)

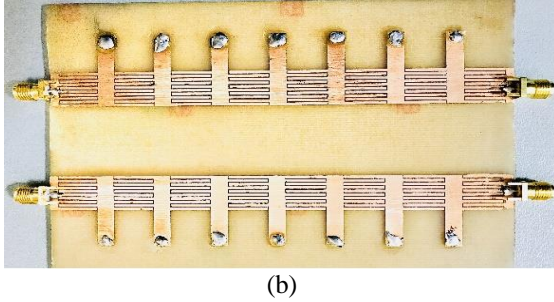


Fig. 5. Photographs of the printed microstrip seven unit-cells CRLH-CRLH coupler (top layer) for: (a) case 1 and (b) case 2.

Table 3: Cross-correlation metric for similarity determination

| | Data 1 for Case 1 | | Data 2 for Case 2 | |
|--------------------------------|-------------------|-----------------|-------------------|-----------------|
| | Measured Data | Momentum Method | Measured Data | Momentum Method |
| Correlation Coefficient ρ | 0.972 | 0.974 | 0.97 | 0.974 |

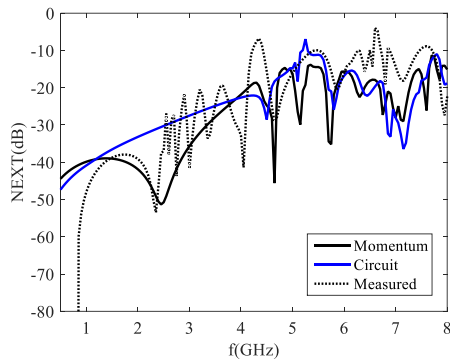


Fig. 6. Measurement and simulation results for case 1 (strong coupling).

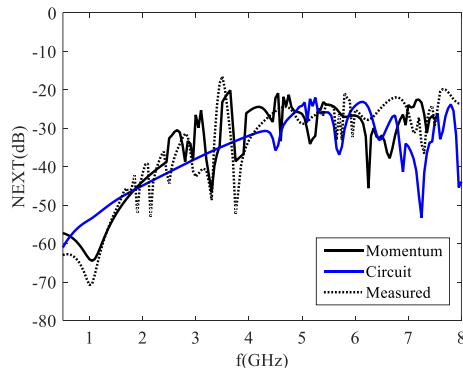


Fig. 7. Measurement and simulation results for case 2 (weak coupling).

V. CONCLUSION

EMC coupling between CRLH transmission lines

has been investigated. Analytical expressions have been derived to compute near- and far-end crosstalk voltages and were validated with the simulation and measurement results for two 7 unit-cells CRLH-CRLH transmission lines. It was shown that using left-handed parameters of CRLH structure, the near and far-end crosstalk voltages can be reduced in left-handed band of the structure. The effects of left-handed capacitance and inductance on left-handed band and crosstalk voltages were discussed.

REFERENCES

- [1] C. Paul, *Introduction to Electromagnetic Compatibility*. John Wiley and Sons, Inc, Hoboken NJ, 2006.
- [2] H. W. Ott, *Electromagnetic Compatibility Engineering*. John Wiley and Sons, Inc, Hoboken NJ, 2009.
- [3] T. Tobana, T. Sasamori, and Y. Isota, "Analysis of electromagnetic coupling between microstrip line and ground slot on a printed circuit board," *Proc. of the International Symposium on Electromagnetic Compatibility - EMC Europe 2016*, Wroclaw, Poland, Sep. 5-9, 2016.
- [4] C. Caloz, A. Sanda, and T. Itoh, "A novel composite right-/left-handed coupled-line directional coupler with arbitrary coupling level and broad bandwidth," *IEEE Transactions on Microwave Theory and Techniques.*, vol. 52, no. 3, pp. 980-992, Mar. 2004.
- [5] I. A. Mocanu, G. I. Sajin, and F. Craciunoiu, "Electromagnetic study of strong coupled CRLH transmission lines for use in antenna construction," *IEEE Asia-Pacific Conference on Antennas and Propagation*, Singapore, Aug. 27-29, 2012.
- [6] A. A. Ibrahim, M. A. Abdalla, and D. Budimir, "Coupled CRLH transmission lines for compact and high selective bandpass filters," *Microwave and Optical Technology Letters*, vol. 59, no. 6, pp. 1248-1251, Mar. 2017.
- [7] Irfanullah, S. Nariyal, S. Roy, M. M. Masud, B. Ijaz, and B. D. Braaten, "Analysis of the noise voltage coupling (crosstalk) between right-handed and composite right/left-handed (CRLH) transmission lines on printed circuit boards," *IEEE Trans. Electromn. Compat.*, vol. 55, no. 4, pp. 788-797, Aug. 2013.
- [8] B. Ijaz, S. Roy, M. M. Masud, A. Iftikhar, S. Nariyal, Irfan Ullah, K. Asirvatham, B. Booth, and B. D. Braaten, "A series-fed microstrip patch array with interconnecting CRLH transmission lines for WLAN applications," *7th European Conference on Antennas and Propagation (EuCAP)*, Gothenburg, pp. 2088-2091, Apr. 8-12, 2013.
- [9] M. S. Khan, A.-D. Capobianco, A. Iftikhar, S. Asif, B. Ijaz, and B. D. Braaten, "A frequency-reconfigurable series-fed microstrip patch array

- with interconnecting CRLH transmission lines,” *IEEE Antennas and Wireless Propagation Letters*, vol. 15, pp. 242-245, June 2016.
- [10] A. Lai, K. M. K. H. Leong, and T. Itoh, “Novel series divider for antenna arrays with arbitrary element spacing based on a composite right/left-handed transmission line,” *European Microwave Conference*, Paris, Oct. 4-6, 2005.
- [11] J. M. Kovitz, Y. R. Samii, and J. Choi, “Dispersion engineered right/left-handed transmission lines enabling near-octave bandwidths for wideband CP patch arrays,” *IEEE International Symposium on Antennas and Propagation & USNC/URSI National Radio Science Meeting*, Vancouver, BC, July 19-24, 2015.
- [12] T. Tsukagoshi, K. Fujimori, M. Sanagi, and S. Nogi, “A metamaterial mirror with multiple CRLH transmission lines and its imaging quality,” *Proceedings of the 39th European Microwave Conference*, Rome, Sep. 29-Oct. 1, 2009.
- [13] C. Caloz and T. Itoh, *Electromagnetic Metamaterials: Transmission Line Theory and Applications*. John Wiley and Sons, Inc, Hoboken NJ, pp. 124-128, 2006.
- [14] B. D. Braaten, S. Roy, I. Ullah, S. Nariyal, B. Ijaz, M. M. Masud, S. A. Naqvi, and A. Iftikhar, “A cascaded reconfigurable RH/CRLH zero-phase microstrip transmission line unit cell,” *Proceedings of the IEEE Intern. Conf. on Wireless Infor. Tech. and Systems*, Maui, Hawaii, Nov. 11-16, 2012.
- [15] N. Kou, Y. Shi, and L. Li, “New equivalent circuit analysis and synthesis for broadband composite right/left-handed transmission line metamaterials,” *ACES Journal*, vol. 31, no. 8, Aug. 2016.
- [16] N. Soleimani, Mohammad G. H. Alijani, and Mohammad H. Nishati, “Crosstalk analysis of uniform and nonuniform lossy microstrip-coupled transmission lines,” *International Journal of RF and Microwave Computer-Aided Engineering*, vol. 29, no. 11, July 2019.
- [17] Y. Sun, J. Wang, W. Song, and R. Xue, “Frequency domain analysis of lossy and non-uniform twisted wire pair,” *IEEE Access*, vol. 7, Apr. 2019.
- [18] X. Liu, Y. Li, and L. Zhao, “Investigation and analysis on crosstalk of the parallel meander transmission lines,” *ACES Conf.*, Beijing, July 29-Aug. 1, 2018.
- [19] Y. X. Sun, Q. Li, W. H. Yu, Q. H. Jiang, and Q. K. Zhuo, “Study on crosstalk between space transient interference microstrip lines using finite difference time domain method,” *ACES Journal*, vol. 30, no. 8, Aug. 2015.